



HAL
open science

Kinetics and Products of the Reaction of OH Radicals with ClNO from 220 to 940 K

Yuri Bedjanian

► **To cite this version:**

Yuri Bedjanian. Kinetics and Products of the Reaction of OH Radicals with ClNO from 220 to 940 K. *Journal of Physical Chemistry A*, 2018, 122 (4), pp.916-922. 10.1021/acs.jpca.7b11946 . hal-02117979

HAL Id: hal-02117979

<https://hal.science/hal-02117979v1>

Submitted on 21 Nov 2019

HAL is a multi-disciplinary open access archive for the deposit and dissemination of scientific research documents, whether they are published or not. The documents may come from teaching and research institutions in France or abroad, or from public or private research centers.

L'archive ouverte pluridisciplinaire **HAL**, est destinée au dépôt et à la diffusion de documents scientifiques de niveau recherche, publiés ou non, émanant des établissements d'enseignement et de recherche français ou étrangers, des laboratoires publics ou privés.

**Kinetics and Products of the Reaction of OH Radicals with CINO
from 220 to 940K**

Yuri Bedjanian*

Institut de Combustion, Aérodynamique, Réactivité et Environnement (ICARE), CNRS
45071 Orléans Cedex 2, France

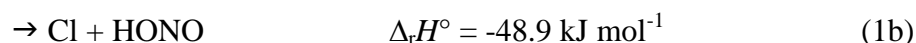
*Corresponding author: Tel.: +33 238255474, Fax: +33 238696004, e-mail: yuri.bedjanian@cnrs-orleans.fr

ABSTRACT

The kinetics and products of the reaction of OH radicals with ClNO have been studied in a flow reactor coupled with an electron impact ionization mass spectrometer at nearly 2 Torr total pressure of helium and over a wide temperature range, $T = 220 - 940$ K. The rate constant of the reaction $\text{OH} + \text{ClNO} \rightarrow \text{products}$ (1) was determined under pseudo-first order conditions, monitoring the kinetics of OH consumption in excess of ClNO: $k_1 = 1.48 \times 10^{-18} \times T^{2.12} \exp(146/T) \text{ cm}^3 \text{ molecule}^{-1} \text{ s}^{-1}$ (uncertainty of 15%). HOCl, Cl and HONO were observed as the reaction products. As a result of quantitative detection of HOCl and Cl, the partial rate constants of the HOCl + NO (1a) and Cl + HONO (1b) forming reaction pathways were determined in the temperature range 220-940K: $k_{1a} = 3.64 \times 10^{-18} \times T^{1.99} \exp(-114/T)$ and $k_{1b} = 4.71 \times 10^{-18} \times T^{1.74} \exp(246/T) \text{ cm}^3 \text{ molecule}^{-1} \text{ s}^{-1}$ (uncertainty of 20%). The dynamics of the title reaction and, in particular, non-Arrhenius behavior observed for both k_{1a} and k_{1b} in a wide temperature range, seems to be an interesting topic for theoretical research.

1. INTRODUCTION

Reaction of OH radicals with ClNO is an interesting subject for a kinetic study in a wide temperature range, as a reaction proceeding via two competing pathways with comparable branching ratios and non-Arrhenius curved temperature dependence of the rate constant:



The thermochemical data used for the calculations of $\Delta_r H^\circ$ are from ref. 1. Previous studies²⁻⁵ of this reaction were motivated by atmospheric implications and kinetic interest: the possibility to use this reaction as a source of HOCl, important atmospheric species, in laboratory studies;² determination of the atmospheric lifetime of ClNO toward its reaction with OH;³⁻⁴ study of a homologous series of the reactions of ClNO with a series of radicals focused on the understanding of the reaction mechanism.⁵ With regard to the atmospheric fate of ClNO, it has been shown in particular that reaction with OH is too slow to compete with the fast photolysis of ClNO.⁴ Rate constant of reaction 1 has been measured in three previous studies:^{2,4-5} at $T = 298\text{K}$ by Poulet et al.,² and by Finlayson-Pitts et al.⁴ and Abbatt et al.⁵ in the temperature range 262-368 K and 217-424 K, respectively. Room temperature value of k_1 reported by Poulet et al.² is in good agreement with the results of Abbatt et al.,⁵ while the results from two temperature dependence studies⁴⁻⁵ differ up to 30%. In addition, Abbatt et al.,⁵ have observed a nonlinear Arrhenius behavior of k_1 which would be interesting to examine at higher temperatures. Poulet et al.² looking for the products of reaction 1, have shown that reaction proceeds through two competing pathways, Cl-atom abstraction channel and HONO + Cl forming one with similar (close to 50%) branching ratios at room temperature. Finlayson-Pitts et al.⁴ following by mass spectrometry the ratio of the relative signals corresponding to the species formed in reactions 1a (HOCl) and 1b (Cl), concluded that the branching ratios for two reactive channels are independent of temperature in the range

262-368K. This observation is in contradiction with the interpretation of the nonlinear Arrhenius behavior of k_1 proposed by Abbatt et al.⁵ and seems to clearly indicate the need of the data on the yield of the reaction products in a wide temperature range.

In the present work we report the results of an experimental study of the reaction of OH radicals with ClNO in an extended temperature range, including the measurements of the rate constant and the branching ratio for two reactive pathways as a function of temperature between 220 and 940 K.

2. EXPERIMENTAL

Experiments were carried out in a discharge flow reactor using a modulated molecular beam mass spectrometer with electron impact ionization (Balzers, QMG 420) as the detection method.⁶⁻⁷ Two flow reactors were used in the present work. The first one, a Pyrex tube (45 cm length and 2.4 cm i.d.) with a jacket for the thermostated liquid circulation (water or ethanol),⁶⁻⁷ was employed at low temperatures (220 – 325K) of the study. The walls of the reactor as well as of the movable injector of OH radicals were coated with halocarbon wax (Halocarbon Products Corporation, series 1500) in order to minimize their heterogeneous loss. The second flow reactor, used in the experiments at $T = 298 - 940$ K, consisted of an electrically heated Quartz tube (GE 214, 45 cm length and 2.5 cm i.d.) with water-cooled extremities (Figure S1, Supporting Information).⁸ Temperature in the reactor was measured with a *K*-type thermocouple positioned in the middle of the reactor in contact with its outer surface. Temperature gradients along the flow tube measured with a thermocouple inserted in the reactor through the movable injector was found to be less than 1%.⁸

OH was produced in the movable injector through a rapid reaction of H atoms with excess NO₂ ($[\text{NO}_2] = (1-3) \times 10^{13}$ molecule cm⁻³), hydrogen atoms being generated in a microwave discharge of H₂/He mixtures (Figure S1):



$$k_2 = (1.5 \pm 0.5) \times 10^{-10} \text{ cm}^3 \text{ molecule}^{-1} \text{ s}^{-1} \text{ (T = 195 – 1990 K).}^9$$

OH radicals were detected at $m/z = 96/98$ (HOBr^+) after being scavenged with an excess of Br_2 (added in the end of the reactor 5 cm upstream of the sampling cone, as shown in Figure S1) through reaction 3:



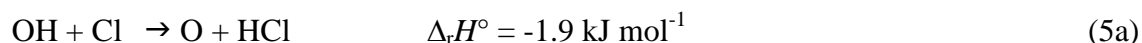
$$k_3 = (1.85 \times 10^{-9}) \times T^{0.66} \text{ cm}^3 \text{ molecule}^{-1} \text{ s}^{-1} \text{ (T = 297 – 766 K).}^{10}$$

This reaction was also used for the determination of the absolute concentrations of OH: $[\text{OH}] = [\text{HOBr}] = \Delta[\text{Br}_2]$, i.e. concentration of OH (HOBr) was determined from the consumed fraction of $[\text{Br}_2]$. Similarly, the reaction of OH radicals with Cl_2 was used to determine the absolute concentrations of HOCl , one of the products of the title reaction:



$$k_4 = 3.6 \times 10^{-16} T^{1.35} \exp(-745/T) \text{ cm}^3 \text{ molecule}^{-1} \text{ s}^{-1} \text{ (T = 297 – 826 K).}^{11}$$

In these calibration experiments, Br_2 was added at the end of the reactor and concentration of HOCl was determined from the consumed fraction of OH (detected as HOBr) upon addition of Cl_2 in the main reactor: $[\text{HOCl}] = \Delta[\text{HOBr}]$. It can be noted that possible secondary reaction of Cl atoms with OH,



seems to be too slow under experimental conditions (low $[\text{OH}]$ and, consequently, $[\text{Cl}]$) of the study to have a significant impact on the results of the measurements. To our knowledge, there are no experimental data on the rate constant of this reaction; only an estimation for k_{5b} based on the rate constant of the reverse reaction and calculated equilibrium constant is available: $k_{5b} = 9.8 \times 10^{-12} \exp(-2860/T) \text{ cm}^3 \text{ molecule}^{-1} \text{ s}^{-1}$.¹² Anyway, in experiments on calibration of HOCl similar results were observed with initial concentration of OH varied by a

factor of 3, which also points to an insignificant role of the reaction (5). Absolute concentrations of ClNO, Cl₂, NO₂ and Br₂ in the reactor were calculated from their flow rates obtained from the measurements of the pressure drop of their mixtures in He stored in calibrated volume flasks. The flow rates of helium, used as a carrier gas, were measured and controlled by flow meters (MKS Instruments).

The purities of the gases used were as follows: He >99.9995% (Alphagaz), passed through liquid nitrogen trap; H₂ > 99.998% (Alphagaz); Br₂ >99.99% (Aldrich); NO₂ > 99% (Alphagaz); Cl₂ > 99.6% (Alphagaz); ClNO ≥ 97% (Matheson).

3. RESULTS AND DISCUSSION

3.1. Rate Constant of Reaction 1. The rate constant of reaction 1 was determined under pseudo-first order conditions from kinetics of OH-radical consumption in high excess of ClNO. The initial concentration of OH radicals was in the range $(2 - 3) \times 10^{11}$ molecule cm⁻³, the concentrations of ClNO are shown in Table 1. The flow velocity in the reactor was in the range (1370-2760) cm s⁻¹. All the measurements were carried out at nearly 2 Torr total pressure of helium which was measured in the center of the reaction zone, pressure gradient in the reactor did not exceed 3%.

Table 1. Reaction OH + ClNO: Summary of the Measurements of the Rate Constant.

<i>T</i> (K)	number of kinetic runs	[ClNO] (10 ¹⁴ molecule cm ⁻³)	<i>k</i> ₁ ^{<i>a</i>} (10 ⁻¹³ cm ³ molecule ⁻¹ s ⁻¹)	reactor ^{<i>b</i>} surface
220	9	0.48-3.42	2.71	HW
232	8	0.47-3.74	2.90	HW
249	8	0.29-5.06	3.17	HW
275	9	0.21-4.39	3.76	HW
299	9	0.40-6.01	4.36	Q
325	8	0.27-2.88	4.81	HW
363	9	0.33-5.34	5.79	Q
400	8	0.23-3.17	7.01	Q
445	8	0.25-3.56	8.41	Q

500	8	0.20-2.13	10.8	Q
571	9	0.12-2.72	13.6	Q
667	8	0.10-1.86	18.3	Q
800	9	0.14-1.38	25.4	Q
940	8	0.07-1.08	34.3	Q

^a Estimated uncertainty on k_1 is 15 %. ^b HW: halocarbon wax; Q: quartz.

Examples of the exponential decays of OH radicals observed at different concentrations of ClNO are shown in Figure 1.

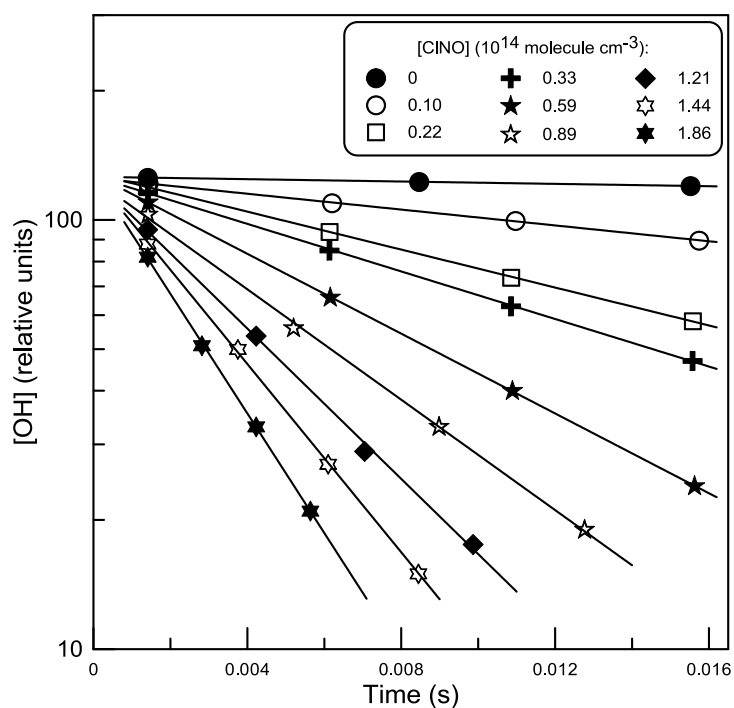


Figure 1. Examples of OH consumption kinetics observed with different concentrations of ClNO at $T = 667$ K.

Figure 2 shows the pseudo-first order rate constant, $k_1' = k_1[\text{ClNO}] + k_w$, as a function of the concentration of ClNO observed at six temperatures between $T = 220$ and 940 K.

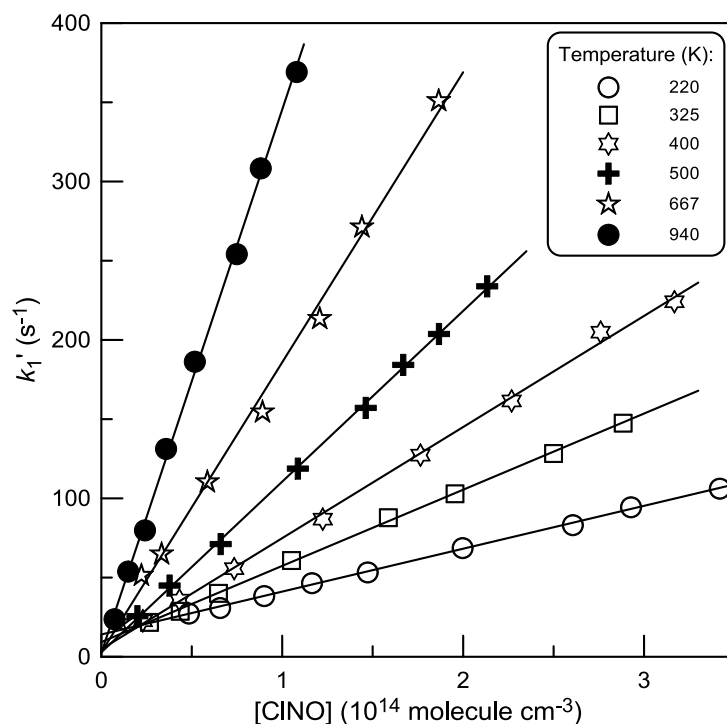


Figure 2. Example of pseudo-first order plots obtained from OH decay kinetics in excess of ClNO at different temperatures in the reactor.

Pseudo-first order plots measured at other temperatures are shown in Figures S2-S3 (Supporting Information). k_w represents the rate of OH decay in the absence of ClNO in the reactor and was measured in separate experiments (example in Figure 1 for [ClNO] = 0). All the measured values of k_1' were corrected for axial and radial diffusion of OH radicals.¹³ The diffusion coefficient of OH in He was calculated as $D_0 = 640 \times (T/298)^{1.85} \text{ Torr cm}^{-2} \text{ s}^{-1}$.¹⁴⁻¹⁵ Corrections on k_1' were less than 10%. The slopes of the straight lines in Figures 2 and S2-S3 provide the values of k_1 at respective temperatures. The intercepts were in the range (1 - 15) s⁻¹, in good agreement with OH loss rate measured in the absence of ClNO in the reactor, with a slight trend to decrease with increasing temperature observed both in the quartz reactor and the Pyrex one covered with halocarbon wax.

All the results obtained for k_1 at different temperatures are shown in Table 1 and Figure 3 (black filled circles). The combined uncertainty on the measurements of the rate constants was estimated to be $\leq 15\%$, including statistical error (within a few percent) and those on the

measurements of the flows (5%), pressure (3%), temperature (1%) and absolute concentration of ClNO ($\leq 10\%$). As one can see, the temperature dependence of k_1 deviates from a simple Arrhenius behavior as could be expected considering that the overall rate constant is the sum of those of two reaction pathways and dependence on temperature of the pre-exponential factors which can be quite noticeable in the wide temperature range used in the study. The experimental data for k_1 were fitted with a three-parameter expression, leading to the following result (continuous line in Figure 3):

$$k_1 = 1.48 \times 10^{-18} \times T^{2.12} \exp(146/T) \text{ cm}^3 \text{ molecule}^{-1} \text{ s}^{-1},$$

with conservative independent of temperature 15% uncertainty on the rate constant.

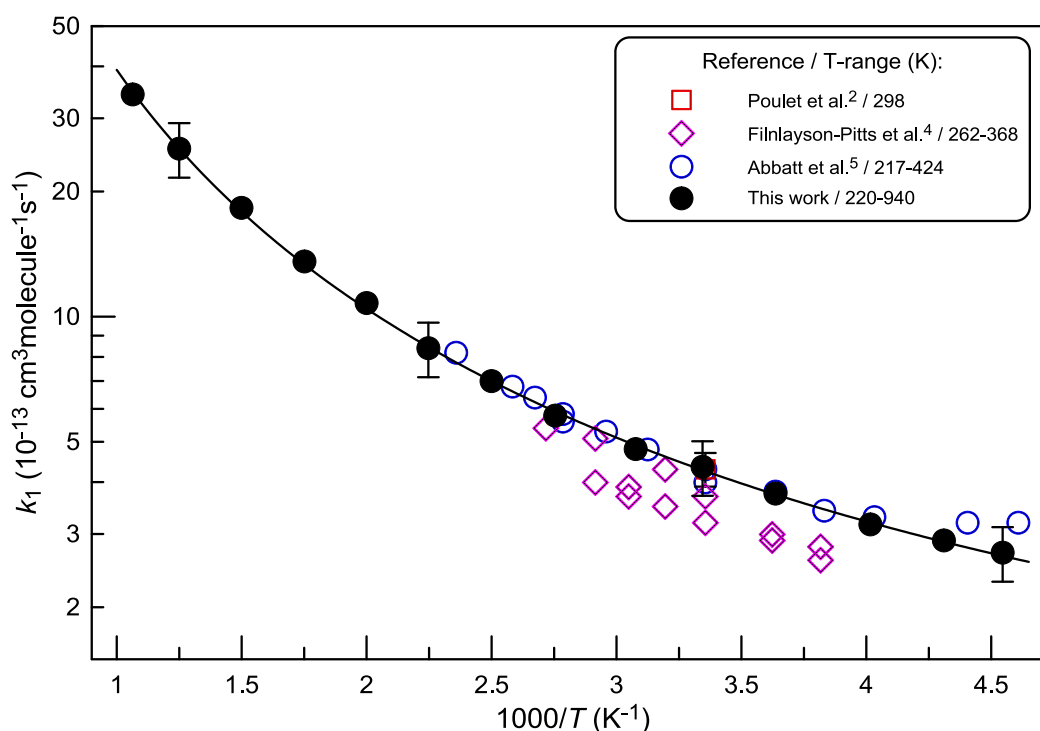


Figure 3. Temperature dependence of the rate constant of the reaction OH + ClNO. Error bars correspond to estimated 15% uncertainties on the determination of k_1 in the present study.

3.2. Products of reaction 1. Like kinetic study above, the products of reaction (1) were explored upon consumption of OH in an excess of ClNO. HOCl and HONO, formed in reactions (1a) and (1b), respectively, were directly observed at their parent peaks at $m/z = 52$

(HOCl⁺) and m/z = 47 (HONO⁺). Cl-atom, co-product of HONO in reaction (1b), once formed, is rapidly consumed in reaction with ClNO, present in high concentrations in the reactor:



$$k_6 = 6.6 \times 10^{-11} \exp(128/T) \text{ cm}^3 \text{ molecule}^{-1} \text{ s}^{-1} \text{ (T = 208 – 373 K).}^5$$

Cl₂ was detected with mass spectrometer at m/z = 70 (Cl₂⁺). Considering the rather complex procedure of synthesis of pure samples of HONO and measurements of their absolute concentrations in a flow reactor,¹⁶ the absolute measurements of the branching ratios for two channels of reaction 1 were carried out with HOCl (channel 1a) and Cl (channel 1b), detected as Cl₂). Experiments on the determination of the yields of the reaction products were carried out with concentration of ClNO in the range (0.9 – 2.8)×10¹⁴ molecule cm⁻³ and reaction time of (0.02 – 0.05) s, and consisted in the measurements of the consumed concentration of OH and formed concentrations of the products. The consumed concentration of OH radicals (> 90% in all the experiments) was corrected for contribution of the heterogeneous loss of OH (1-10%). Example of the experimental data observed at T = 220 and 737 K is shown in Figure 4. Similar data observed at other temperatures of the study are shown in Figures S4-S5 (Supporting Information). The slopes of the straight lines in Figures 4, S4-S5 provide the branching ratios for HOCl (k_{1a}/k_1) and chlorine atom (k_{1b}/k_1) forming pathways of reaction 1 at different temperatures which are shown in Table 2. Estimated systematic uncertainty on the measurements of k_{1a}/k_1 and k_{1b}/k_1 is around 15% and is mainly due to the precision of the measurements of the absolute concentrations of the respective species.

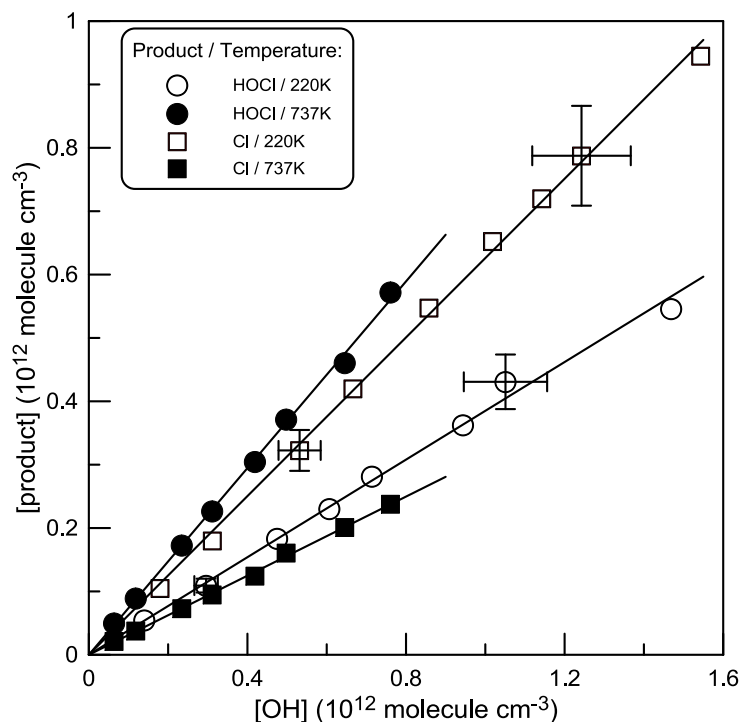


Figure 4. Concentrations of HOCl and Cl formed in reaction (1) as a function of the consumed concentration of OH radicals. Error bars correspond to typical 10% uncertainties on the determination of the absolute concentrations of the relevant species. Continuous lines represent linear through origin fit to the experimental data.

Table 2. Experimental Conditions and Results of the Measurements of the Yields of HOCl (k_{1a}/k_1) and Cl-atom (k_{1b}/k_1).

T (K)	Number of experiments	$[OH]_0$ (10^{12} molecule cm^{-3})	k_{1a}/k_1	k_{1b}/k_1	total ^a
220	8	0.18-1.78	0.384	0.626	1.010
232	9	0.17-1.63	0.389	0.620	1.009
249	9	0.16-1.76	0.411	0.626	1.037
275	9	0.21-1.91	0.443	0.574	1.017
298	7	0.20-1.98	0.495	0.494	0.989
325	8	0.18-1.51	0.513	0.488	1.001
363	9	0.13-1.67	0.544	0.420	0.964
443	9	0.10-1.31	0.621	0.380	1.001
571	9	0.15-1.24	0.691	0.354	1.045
737	8	0.07-0.79	0.732	0.312	1.044
940	9	0.05-0.43	0.765	0.255	1.020

^a Sum of the yields of the two reaction products.

It should be noted that in all the experiments on detection of Cl_2 , the contribution of Cl_2 impurity in CINO (measured to be less than 0.1%) was taken into account. At highest temperature of the study ($T = 940\text{K}$) we have observed production of Cl_2 even in the absence of OH radicals in the reactive system, which was attributed to the thermal decomposition of CINO followed by reaction of the formed Cl atoms with CINO:



Although the decomposition of CINO was insignificant (<10%), the resulting concentration of Cl_2 was rather high compared with those from OH + CINO reaction, preventing the measurements of Cl yield in reaction 1 at $T = 940\text{K}$. The value of k_{1b}/k_1 at $T = 940\text{K}$ presented in Table 2 was determined as a result of the relative measurements of HONO formation in reaction 1b at two temperatures, $T = 298$ and 940 K (Figure 5).

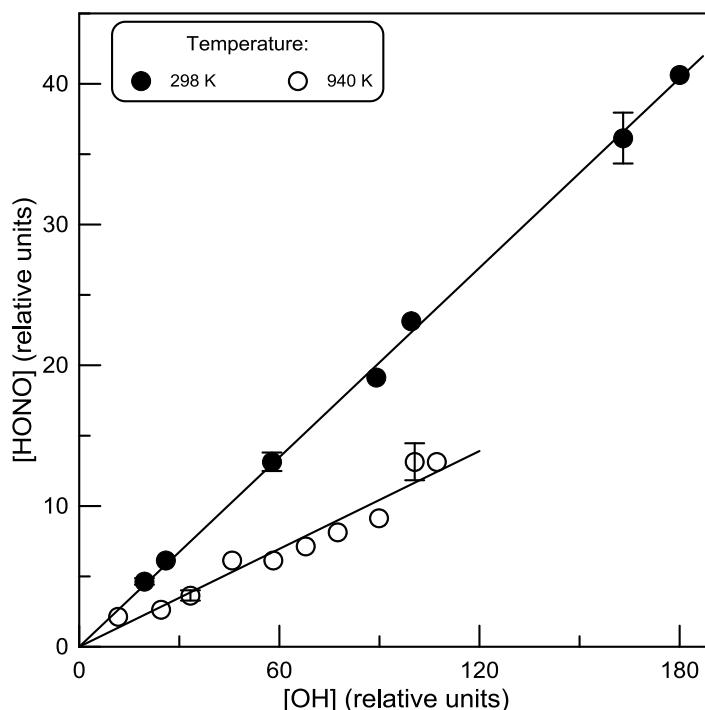


Figure 5. Concentration of HONO formed in reaction (1) as a function of the consumed concentration of OH. Error bars correspond to typical (5-10)% uncertainties on the measurements of HONO signals at $m/z = 47$. Continuous lines represent linear through origin fit to the experimental data.

Using the ratio of slopes of the straight lines in Figure 5, corresponding to the data at room temperature and $T = 940\text{K}$ and equal to 1.94, and the value of $k_{1b}/k_1 = 0.494$ measured at $T = 298\text{ K}$ upon detection of Cl_2 , one gets the value of $k_{1b}/k_1 = 0.255$ at $T = 940\text{K}$.

All the branching ratio data obtained for reaction 1 are shown in Figure 6. As one can see, an increase of k_{1a}/k_1 (Cl-atom abstraction channel) and decrease of k_{1b}/k_1 (OH addition / Cl elimination channel) with increasing temperature is observed.

The rate constants of two channels of reaction 1 calculated using the measured branching ratio data and the expression for total rate constant derived above, $k_1 = 1.48 \times 10^{-18} \times T^{2.12} \exp(146/T) \text{ cm}^3 \text{ molecule}^{-1} \text{ s}^{-1}$, are shown in Figure 7. The solid lines result from the nonlinear least-squares analysis of all the experimental data for k_{1a} , k_{1b} and total rate constant in accordance with $k_1 = k_{1a} + k_{1b}$ and three-parameter expressions for k_{1a} and k_{1b} :

$$k_{1a} = 3.64 \times 10^{-18} \times T^{1.99} \exp(-114/T) \text{ cm}^3 \text{ molecule}^{-1} \text{ s}^{-1},$$

$$k_{1b} = 4.71 \times 10^{-18} \times T^{1.74} \exp(246/T) \text{ cm}^3 \text{ molecule}^{-1} \text{ s}^{-1},$$

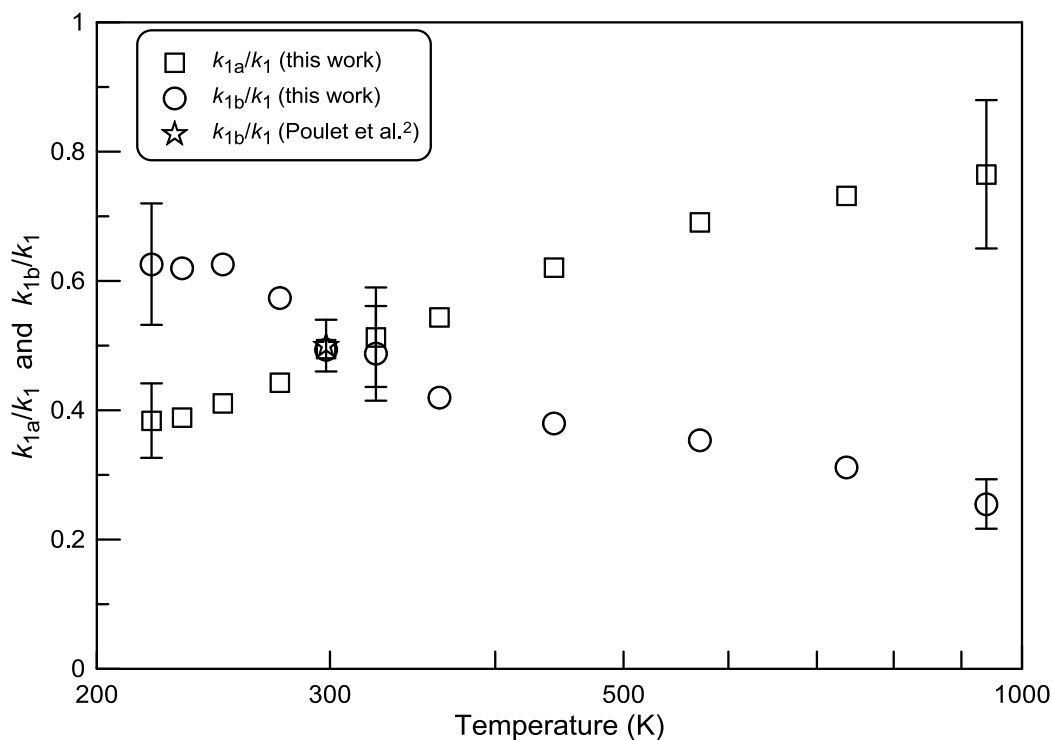


Figure 6. Branching ratios for two channels of reaction 1 as a function of temperature. The error bars show the estimated 15 % and 1σ uncertainty on the present measurements and those of Poulet et al.,² respectively.

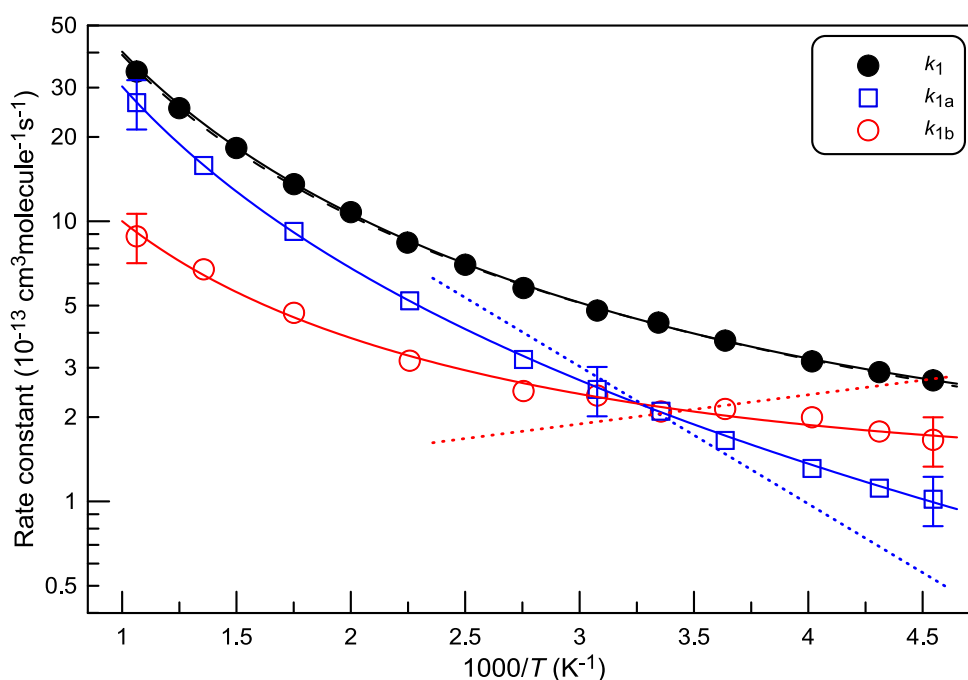


Figure 7. Total rate constant and those for two channels of reaction 1 as a function of temperature. The error bars represent estimated 20 % uncertainty on the measurements of k_{1a} and k_{1b} . Blue and red dotted lines correspond to k_{1a} and k_{1b} estimated in reference 5.

The conservative estimated uncertainty on k_{1a} and k_{1b} is 20% and includes the uncertainties on the measurements of the respective branching ratios and total rate constant. It can be noted that two presentations of the total rate constant, according to the expression for k_1 derived above (dashed line in Figure 7) and as a sum of the three-parameter expressions for k_{1a} and k_{1b} (solid line in Figure 7), are practically indistinguishable.

3.3. Comparison with previous data. Rate constant of reaction 1 has been measured in three previous studies (see Figure 5).^{2,4-5} Poulet et al.² using discharge flow reactor with EPR detection of OH radicals measured $k_1 = (4.3 \pm 0.4) \times 10^{-13} \text{ cm}^3 \text{ molecule}^{-1} \text{ s}^{-1}$ (with $\pm 2\sigma$ uncertainty) at $T = 298\text{K}$ and total pressure of 0.5-1 Torr. Abbatt et al.⁵ measured the rate constant of reaction 1 in a discharge flow reactor at $T = 217\text{-}424 \text{ K}$ and total pressure of 1 - 2 Torr using resonance fluorescence and laser magnetic resonance methods for detection of OH. As one can see in Figure 3, the values of k_1 reported previously by Poulet et al.² and Abbatt et

al.⁵ are in excellent agreement with the present data. The values of k_1 reported by Finlayson-Pitts et al.⁴ are somewhat lower, however, consistent with all of the data. Finlayson-Pitts et al.⁴ have used three different coatings, boric acid, phosphoric acid, and halocarbon wax, of the flow tube in their experiments. In the boric acid coated reactor they have found an evidence for the heterogeneous reaction occurring at temperatures below 298K. That is why only the results obtained with phosphoric acid and halocarbon wax are presented in Figure 3. It can be noted that in the present work, we have not observed any heterogeneous complications: similar results were obtained in quartz and halocarbon wax coated reactors (Table 1).

Products of reaction 1 were quantified in only previous study of Poulet et al.² who reported the branching ratio of 0.50 ± 0.04 for the channel 1b which is in excellent agreement with the present data (Table 2 and Figure 6). Finlayson-Pitts et al.⁴ measured the ratio of the peak heights of HOCl and Cl₂, corresponding to the products of reactions 1a and 1b, as a function of total pressure (0.2-0.8 Torr) and temperature (276, 298 and 353 K). Within experimental error ($\approx 20\%$), no significant change in the ratio of the peak heights of HOCl to Cl₂ was observed. This observation is not supported by the present data showing an increase in the ratio of the yields of HOCl to Cl by a factor of nearly 1.5 in the temperature range 276 – 353 K.

Abbatt et al.,⁵ using the branching ratio reported by Poulet et al.² at $T = 298\text{K}$ and assuming that the abstraction channel is minor at low temperatures, estimated the temperature dependences of the two channels of reaction 1: $k_{1a} = 9.0 \times 10^{-12} \exp(-1130/T) \text{ cm}^3 \text{ molecule}^{-1} \text{ s}^{-1}$ and $k_{1b} = 9.2 \times 10^{-14} \exp(240/T) \text{ cm}^3 \text{ molecule}^{-1} \text{ s}^{-1}$. k_{1a} and k_{1b} corresponding to these expressions are shown in Figure 7 as blue and red dotted lines, respectively. One can note that the experimental results from the present study do not support the estimated temperature dependences of k_{1a} and k_{1b} : both rate constants are found to increase with temperature with well pronounced non-Arrhenius behavior at $T \geq 400 \text{ K}$. Accordingly, the non-Arrhenius

behavior of the total rate constant is not due only to different temperature dependences for the two reaction channels, as was supposed by Abbatt et al.,⁵ but also due to non-Arrhenius behavior of both partial rate constants. The increase of upward curvature of k_{1a} and k_{1b} with temperature can be caused by temperature dependence of the pre-exponential factors (collision and transition state theoretical pre-exponential factors are proportional to the square root of and to temperature, respectively) and activation energy.¹⁷ It should also be noted that reaction 1b is a complex one and is expected to proceed via formation of an intermediate complex which can decompose either to final reaction products, Cl and HONO, or back to reactants. It is clear that theoretical high level calculations would be very beneficial to understand the dynamics of this reaction and identify its specific features leading to the experimental observations reported in this study.

CONCLUSIONS

In this work, we investigated the kinetics and products of the reactions of OH radicals with ClNO using a low pressure flow reactor coupled to an electron impact ionization mass spectrometer. The total rate constant of the reaction determined in the temperature range (220 – 940) K and found to be in good agreement with previous measurements at lower temperatures, $k_1 = 1.48 \times 10^{-18} \times T^{2.12} \exp(146/T) \text{ cm}^3 \text{ molecule}^{-1} \text{ s}^{-1}$, is recommended from the present study. Three products, HOCl, Cl and HONO, of the two major channels of the title reaction, HOCl + NO (1a) and Cl + HONO (1b), were identified. As a result of quantitative measurements of HOCl and Cl, the rate constants for the two reaction pathways were determined at $T = 220 - 940 \text{ K}$ as: $k_{1a} = 3.64 \times 10^{-18} \times T^{1.99} \exp(-114/T)$ and $k_{1b} = 4.71 \times 10^{-18} \times T^{1.74} \exp(246/T) \text{ cm}^3 \text{ molecule}^{-1} \text{ s}^{-1}$. The observed non-Arrhenius behavior of k_{1a} and k_{1b} can be due to temperature dependence of the Arrhenius parameters, pre-exponential factor and activation energy, and to a complex nature of the reaction 1b. In order to clarify these points

and better understand the dynamics of the title reaction theoretical high level calculations would be very welcome.

ACKNOWLEDGEMENT

Financial support from CNRS is gratefully acknowledged.

Supporting Information. Diagram of the flow reactor (Figure S1); pseudo-first order plots obtained from OH decay kinetics in excess of ClNO at different temperatures (Figures S2-S3); concentration of HOCl formed in reaction OH + ClNO as a function of the consumed concentration of OH radicals at different temperatures (Figure S4); concentration of Cl formed in reaction OH + ClNO as a function of the consumed concentration of OH radicals at different temperatures (Figure S5).

REFERENCES

- (1) Burkholder, J. B.; Sander, S. P.; Abbatt, J.; Barker, J. R.; Huie, R. E.; Kolb, C. E.; Kurylo, M. J.; Orkin, V. L.; Wilmouth, D. M.; Wine, P. H. Chemical Kinetics and Photochemical Data for Use in Atmospheric Studies, Evaluation No. 18, JPL Publication 15-10, Jet Propulsion Laboratory. <http://jpldataeval.jpl.nasa.gov> (accessed December 2017).
- (2) Poulet, G.; Jourdain, J. L.; Laverdet, G.; Le Bras, G. Kinetic Study of the Reaction of OH Radicals with Nitrosyl Chloride as a Possible Source of ClOH. *Chem. Phys. Lett.* **1981**, *81*, 573-577.
- (3) Finlayson-Pitts, B. J.; Ezell, M. J.; Grant, C. E. Temperature Dependence of the Hydroxyl + Nitrosyl Chloride (ClNO) Reaction: Evidence for Two Competing Reaction Channels. *J. Phys. Chem.* **1986**, *90*, 17-19.
- (4) Finlayson-Pitts, B. J.; Ezell, M. J.; Wang, S. Z.; Grant, C. E. Reaction of Hydroxyl with Nitrosyl Chloride: Kinetics and Mechanisms. *J. Phys. Chem.* **1987**, *91*, 2377-2382.
- (5) Abbatt, J. P. D.; Toohey, D. W.; Fenter, F. F.; Stevens, P. S.; Brune, W. H.; Anderson, J. G. Kinetics and Mechanism of $X + ClNO \rightarrow XCl + NO$ ($X = Cl, F, Br, OH, O, N$) from 220 K to 450 K. Correlation of Reactivity and Activation Energy with Electron Affinity of X. *J. Phys. Chem.* **1989**, *93*, 1022-1029.
- (6) Bedjanian, Y.; Riffault, V.; Le Bras, G.; Poulet, G. Kinetic Study of the Reactions of OH and OD with HBr and DBr. *J. Photochem. Photobiol. A* **1999**, *128*, 15-25.
- (7) Bedjanian, Y.; Le Bras, G.; Poulet, G. Kinetic Study of the Reactions of Br₂ with OH and OD. *Int. J. Chem. Kinet.* **1999**, *31*, 698-704.
- (8) Morin, J.; Romanias, M. N.; Bedjanian, Y. Experimental Study of the Reactions of OH Radicals with Propane, *n*-Pentane, and *n*-Heptane over a Wide Temperature Range. *Int. J. Chem. Kinet.* **2015**, *47*, 629-637.

- (9) Manion, J. A.; Huie, R. E.; Levin, R. D.; Burgess, D. R.; Orkin, V. L.; Tsang, W.; McGivern, W. S.; Hudgens, J. W.; Knyazev, V. D.; Atkinson, D. B., et al. NIST Chemical Kinetics Database, NIST Standard Reference Database 17, Version 7.0 (Web Version), Release 1.6.8, Data Version 2015.12, National Institute of Standards and Technology, Gaithersburg, Maryland, 20899-8320. <http://kinetics.nist.gov/> (accessed December 2017).
- (10) Bryukov, M. G.; Dellinger, B.; Knyazev, V. D. Kinetic Study of the Gas-Phase Reaction of OHh with Br₂. *J. Phys. Chem. A* **2006**, *110*, 9169-9174.
- (11) Bryukov, M. G.; Knyazev, V. D.; Lomnicki, S. M.; McFerrin, C. A.; Dellinger, B. Temperature-Dependent Kinetics of the Gas-Phase Reactions of OH with Cl₂, CH₄, and C₃H₈. *J. Phys. Chem. A* **2004**, *108* (47), 10464-10472.
- (12) Baulch, D. L.; Duxbury, J.; Grant, S. J.; Montague, D. C., Evaluated Kinetic Data for High Temperature Reactions. Volume 4. Homogeneous Gas Phase Reactions of Halogen- and Cyanide-Containing Species. *J. Phys. Chem. Ref. Data* 1981, Supplement No. 1, 10, 723.
- (13) Kaufman, F. Kinetics of Elementary Radical Reactions in the Gas Phase. *J. Phys. Chem.* **1984**, *88*, 4909-4917.
- (14) Bedjanian, Y.; Nguyen, M. L.; Le Bras, G. Kinetics of the Reactions of Soot Surface-Bound Polycyclic Aromatic Hydrocarbons with the OH Radicals. *Atmos. Environ.* **2010**, *44*, 1754-1760.
- (15) Ivanov, A. V.; Trakhtenberg, S.; Bertram, A. K.; Gershenzon, Y. M.; Molina, M. J. OH, HO₂, and Ozone Gaseous Diffusion Coefficients. *J. Phys. Chem. A* **2007**, *111*, 1632-1637.
- (16) Bedjanian, Y.; Lelièvre, S.; Bras, G. L. Kinetic and Mechanistic Study of the F Atom Reaction with Nitrous Acid. *J. Photochem. Photobio. A* **2004**, *168*, 103-108.
- (17) Smith, I. W. M., *Kinetics and Dynamics of Elementary Gas Reactions*. Butterworths: London ; Boston, 1980.

TOC Graphic

